



**One-pot Hydrodeoxygenation (HDO) of Lignin Monomers to
C9 Hydrocarbons co-catalysed by Ru/C and Nb2O5**

Journal:	<i>Green Chemistry</i>
Manuscript ID	GC-ART-05-2020-001692.R1
Article Type:	Paper
Date Submitted by the Author:	01-Sep-2020
Complete List of Authors:	<p>Li, Simin; University of California, Santa Barbara, Department of Chemistry and Biochemistry; State Key Laboratory of Clean Energy Utilization</p> <p>Liu, Baoyuan; University of California, Santa Barbara, Department of Chemistry and Biochemistry</p> <p>Truong, Julianne; University of California, Santa Barbara, Department of Chemistry and Biochemistry</p> <p>Luo, Zhongyang; State Key Laboratory of Clean Energy Utilization, Ford, Peter; University of California, Santa Barbara, Department of Chemistry and Biochemistry</p> <p>Abu-Omar, Mahdi; University of California, Chemistry and Biochemistry, and Chemical Engineering</p>

ARTICLE

One-pot Hydrodeoxygenation (HDO) of Lignin Monomers to C9 Hydrocarbons co-catalysed by Ru/C and Nb₂O₅

Simin Li^{a,b}, Baoyuan Liu^a, Julianne Truong^a, Zhongyang Luo^{*,b}, Peter C. Ford^{*,a}, Mahdi M. Abu-Omar^{*,a}

Received 00th January 20xx,
Accepted 00th January 20xx

DOI: 10.1039/x0xx00000x

A physical mixture of Ru/C and Nb₂O₅ is an effective catalyst for upgrading lignin monomers under low H₂ pressure at 250 °C to a clean cut of hydrocarbon liquid fuel. The reaction solvent is water with a small amount of methanol additive. The hydrodeoxygenation (HDO) was evaluated by using dihydroeugenol (DHE) as an exemplary model lignin monomer. Under optimized conditions, 100% conversion of DHE and very high selectivity to propyl cyclohexane (C9 hydrocarbon) was achieved. The Nb₂O₅ was prepared at low temperature (450 °C) and was shown to contain acid sites that enhance the production of fully deoxygenated product. The methanol additive serves as hydrogen source for the Ru/C catalysed reduction of the aromatic ring. In addition, when a substrate mixture of DHE, isoeugenol and 4-allylsyringol simulating lignin products was employed, 100% conversion to propyl cyclohexane (76%) and propyl benzene (24%) was observed, thereby suggesting the general applicability of this catalyst system for funneling lignin monomers into a clean slate of hydrocarbon liquid fuels. This study sheds light on the function of each catalyst component and provides a simple and green utilization of biomass monomers as a feedstock for renewable hydrocarbon fuels.

Introduction

Non-renewable fossil carbon has been the main resource to produce most chemicals and fuels for the past century; however, renewable alternatives are available. Lignocellulose is by far the most abundant renewable source of non-food-based carbon, and there is considerable interest in upgrading such biomass as a sustainable feedstock.¹⁻⁵ The lignin component of lignocellulose is the second most plentiful biopolymer in nature (after cellulose), has a high carbon content, and is (potentially) the largest renewable resource of aromatic chemicals and fuels.⁵⁻⁹ However, it has an irregular structure with random linkages between monomeric components having different levels of oxygenation that is challenging to utilize chemically.¹⁰ Due to this dilemma, pulp, and paper industries and biorefineries typically dispose of lignin by burning it. Thus, lignin is an attractive target for biomass valorisation.

Lignin can be converted to bio-oil as a renewable liquid fuel.¹¹ However, bio-oils cannot be used in conventional gasoline and diesel fuel engines due to the high oxygen content [up to 60 weight % (wt %)] that makes them immiscible with petroleum-derived fuels.^{12, 13} Thus, oxygen removal while maintaining the carbon structures has the potential to enhance the utilization of bio-oil as a transportation fuel.

Catalytic hydrodeoxygenation (HDO) can upgrade bio-oils. In most studies, HDO involves treatment at high temperatures (250-500 °C) with high pressure of H₂ (50-100 bar). The high pressures required may limit the scalability of the reaction and is a safety hazard.¹⁴ These obstacles encourage the research towards alternative approaches for phenolic upgrading under milder conditions.

The goal of the present study is to develop catalytic strategies that efficiently funnel lignin disassembly components into a narrowly defined product stream useful as a feedstock for the synthesis of aromatic chemicals (C6-C9 aromatic hydrocarbons) or as drop-in biofuels. Phenolics would be desirable for the former processes, while oxygen-free hydrocarbons that can replace fossil-carbon liquid fuels would serve the latter purpose.¹⁵⁻¹⁷ In previous studies, various types of heterogeneous catalysts,¹⁷⁻²⁰ transition metal compounds (phosphides,²¹⁻²⁶ carbides,^{24, 25} and nitrides^{25, 27}), but mainly noble metals (Pt, Pd, Rh, Ru),^{14, 15} have been used, but these require high temperature, and high pressure conditions. For example, Lu et al showed Pd/TiO₂ catalyses with the HDO/hydrogenation of guaiacol to cyclohexane, but this required 30 bar H₂ at 260 °C.²⁸ Kim et al. reported that ruthenium on carbon (Ru/C) converted guaiacol to cyclohexanol with 60% selectivity using the H-donor 2-propanol without added H₂ at 200 °C for 5 h, but the HDO was only partial.²⁹

The use of Niobium Oxide has primarily been studied to show its specific role involved in HDO. Shown in the studies of Wang et al., Nb₂O₅ was primarily used as a catalyst support for Ruthenium to form indane with and without the addition of CH₂Cl₂ as its primary solvent. The main function Nb₂O₅ partook was catalysing the intramolecular cyclization and hydrogenation of lignin oil.⁷ Jiang et

^a Department of Chemistry & Biochemistry, University of California, Santa Barbara, Building 232, Santa Barbara, California, 93106-9510, United States.

^b State Key Laboratory of Clean Energy Utilization, Zhejiang University, Hangzhou, 310027, PR China.

† Footnotes relating to the title and/or authors should appear here.

Electronic Supplementary Information (ESI) available: [details of any supplementary information available should be included here]. See DOI: 10.1039/x0xx00000x

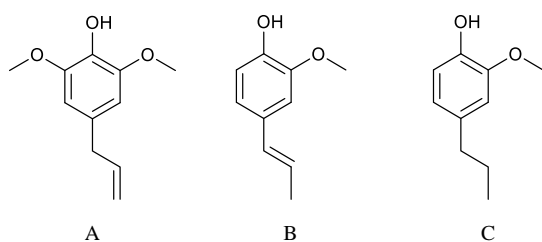


Figure 1. Structures of lignin monomer compounds: (A) 4-allyl-2,6-dimethoxyphenol (4-allylsyringol), (B) isoeugenol, (C) 2-methoxy-4-propylphenol (dihydroeugenol, DHE)

al., utilized Ni/Nb₂O₅ catalyst to produce value-added alcohols from lignin-derived phenols which exhibited selective HDO to give a total alcohol yield of 74%, but requires higher pressure (25 bar H₂).⁸ Puurunen et al., used Pt/Nb₂O₅ to perform HDO on lignin monomer, 4-propylphenol under harsh temperature and pressure (350 °C, 20 bar H₂) to give a selectivity of 77% propylbenzene.⁹ Rinaldi et al., studied Ni/Nb₂O₅ by tuning the acidic and hydrogenating properties of the catalyst to convert lignin to hydrocarbons at 91% yield under 15% catalyst loading and harsh conditions (200 °C, 40 bar H₂).³⁰ Yang et al., reported Nb₂O₅ supported for Pd and Pt where they concluded HDO conversion of lignin to C₇-C₉ products at 42 and 64%, respectively.¹⁸

Described here is the hydroprocessing of dihydroeugenol (DHE) in an aqueous medium using a physical mixture of two catalysts acting synergistically, one is Ru/C, the other is niobium pentoxide (Nb₂O₅). DHE was used as the primary model compound for testing the present catalytic system, since it includes the methoxy, hydroxy, and a propyl groups characteristic of the lignin monomers present in bio-oils (Figure 1). Nb₂O₅ is an air stable, water insoluble white solid that exhibits both strong Lewis and Brønsted acid sites.³¹ It has proved to be an effective catalyst for hydration/dehydration, cracking, condensation, isomerization, and alkylation³²⁻³⁵ as well as for HDO.^{32-34, 36}

The dual catalyst system is effective in hydroprocessing DHE and several other lignin monomers under relatively mild conditions to produce hydrocarbons in high yields. We find that addition of small quantities of methanol (MeOH) as a co-reactant has a significant influence on the product distribution and offer evidence-based mechanistic insight. Furthermore, this system can be tuned to give high selectivity towards hydrocarbon products that can be employed as drop-in fuels.

Experimental

Reagents and Feedstocks

All commercial chemicals were purchased and used as received. 2-Methoxy-4-propylphenol (≥99%), isoeugenol (98%), 2,2-biphenol (99%), and niobium(V) oxide (325 mesh, 99.9%) were purchased from Sigma-Aldrich. Dichloromethane (ACS reagent grade), methanol (ACS Reagent Grade), ethanol (200 Proof), and ethyl acetate (ACS Reagent Grade) were purchased from Fisher Chemical. Cetyltrimethyl ammonium bromide (CTAB, 98%) and

n-dodecane (99%) were purchased from Alfa Aesar. Deuterium oxide (D, 99.9%), and methanol-d₄ (D, 99.8%) were purchased from Cambridge Isotope Laboratories Inc. Propyl benzene (98%) was purchased from Frontier Scientific. Para-cresol (cresylic acid) was purchased from Hercules Powder Company. Hydrochloric Acid (GR ACS) was purchased from EMD Millipore Corporation. Niobium (V) chloride (≥99%) was purchased from Strem Chemicals. Hydrogen gas (5.0 grade) and nitrogen (99.998%) were purchased from Praxair. Water used for reaction and sample preparation was obtained from a A10 Milli-Q water purification system by Millipore.

Catalyst Preparation

Ru/C was obtained from Sigma-Aldrich with 5 wt% Ru loading and used as received. Nb₂O₅ was synthesized using a hydrothermal method according to a modified literature procedure.³⁵ Typically, a 20 mmol portion of the precursor NbCl₅ was dissolved in 20 mL ethanol with rigorous stirring for 10 min, then the solution was added to water solution of CTAB (1 g in 15 mL distilled water) dropwise. The mixed solution was then stirred for 0.5 h followed by adding 20 mL of aqueous HCl (pH 1) that was previously prepared by dissolving a specific amount of hydrochloric acid in water and stirring for another 1.5 h. The resulting sol was then put into a Teflon-lined autoclave and aged at 160 °C for 24 h. Subsequently, the solid was separated and washed with distilled water and dried at 60 °C overnight. After that, the sample was ground and packed for calcination in air. A Thermolyne F6020 1200C Muffle furnace was used to calcinate the niobia sample. Ramping rate of the furnace was pre-set to 1 °C/min. After 6h calcination at 450 °C, the active Nb₂O₅ catalyst was collected at room temperature.

Catalyst Characterization

NH₃-Temperature Programmed Desorption (TPD): To evaluate the acid sites on Nb₂O₅, NH₃-TPD was performed on a Micromeritics AutoChem 2920 instrument. A 200 mg sample of Nb₂O₅ was placed into a U-shaped quartz tube. This material was first pretreated by heating under flowing helium (25 cm³/min) at 300 °C for 0.5 h. A mixture of NH₃ in He (1:9 v/v) was then passed through the tube at a flow rate of 15 cm³/min at 25 °C for 1 h. After that, the sample was flushed with He (25 cm³/min) at 100 °C for another hour. The TPD measurements were carried out over the temperature range 100-500 °C at ramp rate of 10 °C /min and the ammonia concentration in the effluent was monitored with filament thermal conductivity detector (TCD). The amount of desorbed ammonia was determined based on the integrated peak area.

X-ray Diffraction (XRD): The phase structure of Nb₂O₅ was analyzed by powder X-ray diffraction in the diffraction angle 2θ between 10° and 80° on a PANalytical X'Pert PRO X-ray diffractometer with Cu Kα1 radiation (45 kV and 40 mA, k = 1.5406 Å).

Scanning Electron Microscopy (SEM) and Transmission Electron Microscopy (TEM): The particle size and micro morphology of Nb₂O₅ were characterized by scanning electron microscopy (Hitachi SU-8010) at an acceleration voltage of 15

kV. The pore structure of Nb₂O₅ was examined using high-resolution transmission electron microscopy (Tecnai G2 F20 S-TWIN) with the acceleration voltage of 200 kV.

X-ray Photoelectron Spectroscopy (XPS): The niobium oxidation state in the synthesized Nb₂O₅ catalyst was analyzed by X-ray photoelectron spectroscopy (Thermo Scientific K-Alpha+, USA) with a monochromatic radiation source Al K α (12kV, 6mA, 72W). The wide scans were performed with 100 eV pass energy and 1 eV energy step, and the high resolution scans were performed with 30 eV pass energy and 0.1 eV step size. The C1s signal of adventitious carbon (284.8 eV) was used for energy calibration.

Catalytic reaction and product analysis

Reactions in Parr reactor: Batch reactions were carried out in a stainless steel 75 mL 6-series pressure reactor (Parr Instrument Company, 5000 series). The reactor vessel was equipped with magnetic stirring system. For a typical reaction, 0.1 g Ru/C and 0.2 g Nb₂O₅ were physically mixed in the vessel with 12 mL distilled water as solvent. To this were added substrate (0.2 mL) and MeOH (0.8 mL). The reactor was then sealed and purged with H₂ three times. Then, the reactor was filled with H₂ (6 bar). The reactor was heated to 250 °C and held at that temperature for a defined time (typically for 12 h). The stirring rate was kept at 700 rpm during the whole reaction period. Subsequently, the reactor was cooled to room temperature. The products in the liquid phase were extracted using ethyl acetate and the gas phase products were collected in a sealed gasbag for further analysis.

Catalyst Recyclability Test: The recycle experiments were performed in five successive runs with 1 mL DHE loading of each. A physical mixture of fresh Ru/C (0.1 g) and Nb₂O₅ (0.2 g) was employed in the first run. MeOH (1 mL) was then added with 12 mL distilled water as solvent to the reaction mixture in a 75 mL reactor vessel. The reactor was sealed and purged with H₂ three times. Then, the reactor was filled with 11 bar H₂ at room temperature. After that, the reactor was heated to 250 °C and held for 16 h with magnetic stirring at 700 rpm. After reaction, products in liquid phase were extracted using ethyl acetate. The catalyst was washed using ethanol and collected by centrifugation, then dried in a vacuum chamber for 24 h at room temperature. Prior to the next recycle run, the catalyst mixture was heated in an oven at 120 °C for 1 h. The following runs were performed with the same portion of this catalyst mixture collected from the previous run. Turnover number (TON) of each catalyst was calculated based on the total amount of C9 hydrocarbons, i.e. propyl benzene and propyl cyclohexane, produced after the fifth run to show the productivity of each catalyst. The TON was defined and calculated as follows:

$$TON = \frac{\text{total moles of C9 hydrocarbons by 5 runs}}{\text{moles of catalyst}}$$

GC-MS Analysis: A Hewlett-Packard 5890A gas chromatograph (GC) coupled to a Hewlett-Packard 5970B Mass Selective Detector (MSD) was used to identify the products qualitatively. A J&W DB-5 capillary column (30 m x 0.250 mm I.D. x 0.25 μ m film thickness) was installed for analyte

separation. Prior to the injection, the liquid sample was dissolved in ethyl acetate and filtered through a 0.2 micron PTFE syringe filter. The GC injector inlet was set to 280 °C. The oven temperature was held at 50 °C for 2 min. Then the oven was heated to 300 °C at rate of 20 °C per min and held for 10 min. The MSD had a dedicated electron ionization (EI) source and a quadrupole mass analyzer. The mass range of detection was 40 to 550 m/z at a rate of 1.6 scans per second.

GC-FID Analysis: An Agilent 6890N gas chromatograph equipped with a flame ionization detector (FID) was used to quantify the reaction mixtures. A J&W DB-5 GC column (30 m x 0.250 mm I.D. x 0.25 μ m film thickness) was selectively used for separation. The liquid products sample was first passed through a 0.2 micron PTFE syringe filter to remove solid particles, and then diluted to 25 mL in a volumetric flask. A 10 mM n-dodecane solution was pre-made as internal standard for GC quantification. The sample solution was mixed with internal standard (1:1 v/v) in a 2 mL Agilent GC vial. The sample was injected by autosampler. The inlet temperature was kept at 280 °C while the detector temperature was 310 °C. The initial temperature of oven was 40 °C and held for 7 min. Then the oven was heated to 250 °C at ramp rate of 10 °C/min and kept at the final temperature for 5 min. The split mode was used with the split ratio of 10:1. Helium was used as carrier gas at flow rate of 14 mL/min. The instrument was calibrated using the known samples of the products. The analytes were then identified according to their retention time. The quantification of each analyte was acquired from a calibration curve which represented the relationship between concentration versus the ratio of peak area over internal standard.

GC-TCD Analysis: Gas phase products were analyzed by GC-TCD. An Agilent 6890N (G1530N) gas chromatograph equipped with a thermal conductivity detector (TCD) and 30 m x 0.53 mm Fused Silica Carboxen 1010 capillary column was used. The detector was set to 250 °C with H₂ flow at 7 mL/min and air flow at 8 mL/min. The gas phase products were collected in RESTEK polypropylene combo valve gas sampling bag. For each measurement, the 50 μ L gas sample was manually injected by a gastight syringe into the GC inlet at 245 °C. The carrier gas, He, was set to 7 mL/min. The column was pre-heated to 35 °C and held for 5 min. Then the temperature ramped to 245 °C at the rate of 10 °C/min and held for 10 min. Each gas analyte was identified by its retention time.

NMR Analysis: ¹H NMR was obtained by Varian Unity Inova 600 MHz spectrometer. The analyte was extracted by 700 μ L CDCl₃ and packed in glass NMR tube for analysis. ²H NMR was done by using Agilent 400-MR DDR2 400 MHz spectrometer. CHCl₃ with 10% CDCl₃ internal standard was used as the solvent for ²H NMR analysis.

Results

Optimization of dihydroeugenol (DHE) hydrodeoxygenation:

A typical HDO run involved heating a mixture of the model substrate DHE (0.20 mL) with the catalysts Ru/C (100 mg) and Nb₂O₅ (200 mg) added separately, water (12 mL) and a small

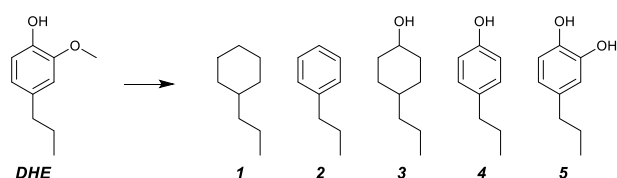


Figure 2. DHE Conversion into five main products: propyl cyclohexane (1), propyl benzene (2), 4-propylcyclohexan-1-ol (3), 4-propylphenol (4), and 4-propylcatechol (5).

amount of MeOH (0.8 mL) in a closed Parr® high pressure reactor that had been flushed with H₂ (P(H₂) = 1 atm at room temperature, RT) then sealed. After a 12 h reaction at 250 °C, the conversion of DHE was 95% (entry 3, Table 1) and of the five potential products shown in Figure 2, the fully deoxygenated hydrocarbons propyl cyclohexane (1) and propyl benzene (2) made up 64% of the product mixture. The balance was mostly the partially deoxygenated product 4-propylcyclohexanol (3). Thus, this catalyst mixture is a promising HDO system. The studies described here were designed to examine the effects of key variables such as MeOH concentration, H₂ pressure, and catalyst loading in order to define those features that may give

Table 1. Performance comparison with different amounts of methanol.

Entry	MeOH (mL)	Conv. (%)	Product Distribution (%)				
			1	2	3	4	5
1 ^a	0	82	3.3	3.5	80	13	-
2 ^b	0.4	80	3.6	9.5	42	45	-
3 ^b	0.8	95	42	22	34	2	-
4 ^b	4	36	8	10	-	24	58
5 ^c	0	0	-	-	-	-	-

Common conditions for each reaction: DHE 0.2 mL, Ru/C 100 mg, Nb₂O₅ 200 mg, H₂O 12 mL, 250 °C, 12 h. Unless noted otherwise, the reactor was first flushed with H₂. ^aInitial P(H₂) at RT = 6 bar (5 bar, gauge). ^bInitial P(H₂) at RT = 1 bar. ^cPurged with nitrogen, no added H₂.

the optimum selectivity toward desired product streams.

Table 1 illustrates the remarkable sensitivity of this system to the amount of methanol added as well as the cooperative requirement for both MeOH and H₂ to obtain the desired HDO products (1) and (2). For example, the reaction with no MeOH but with P(H₂) = 6 bar (RT) (entry 1, Table 1) gave substantial conversion of DHE, but only ~7% of the fully deoxygenated hydrocarbons. In the absence of both H₂ and MeOH, no conversion was observed, and no products were detected (entry 5, Table 1).

Entries 2-4 in Table 1 compare the effect of changing the amount of MeOH added while holding P(H₂) constant at 1 bar (RT). Under these conditions, the optimum amount of MeOH

proved to be 0.8 mL. Surprisingly, raising the MeOH to 4 mL, only about one third the quantity of the aqueous cosolvent, suppressed both the conversion of DHE and the relative amount of HDO products.

Table 2 summarizes the product distributions found for DHE reactions for various P(H₂) (RT) under typical conditions with 0.8 mL MeOH. In the absence of any externally added H₂ (entry 1, Table 2) there was about 64% conversion of DHE, but the only products were the phenol and cyclohexanol derivatives (4) and (3). The amount of conversion increases under increasing H₂ and is 100% when P(H₂) is 6 bar or greater (entries 4-5, Table 2). More importantly, the yield of propyl cyclohexane (1) is 100%. Thus, the latter result requires addition of both MeOH and H₂ and the distribution of HDO products is a function of P(H₂) with

Table 2. Performance with different hydrogen pressures

Entry	P(H ₂) in bar ^a	Conv. (%)	Product Distribution (%)				
			1	2	3	4	5
1 ^b	0	64	-	-	31	69	-
2 ^c	1	95	42	22	34	2	-
3	2	98	53	17	27	3	-
4	6	100	100	-	-	-	-
5	11	100	100	-	-	-	-

Common conditions for each reaction: DHE 0.2 mL, Ru/C 100 mg, Nb₂O₅ 200 mg, H₂O 12 mL, MeOH 0.8 mL, 250 °C, 12 h. Unless noted otherwise, the reactor was first flushed with H₂. ^aInitial P(H₂) at RT. ^bReactor purged with N₂ only, P(N₂) = 1 atm at RT. ^cThe same experiment as entry 3 in Table 1.

high selectivity occurring at a relatively low P(H₂).

Table 3 summarizes experiments with different catalyst mixtures. Interestingly, when the reaction was examined with the addition of Nb₂O₅ alone, the material prepared in this laboratory proved to be much more active than that purchased from a commercial source. The XRD pattern, XPS analysis, SEM and TEM images of the synthesized Nb₂O₅ showed it to be an amorphous, mesoporous catalyst with the niobium in the +5 oxidation state (Supporting information (SI) Figures S-1 and S-2).

The principal reaction in the former case was hydrolysis of the DHE methoxy group to give catechol (5) (entry 1, Table 3) while little activity was seen with the commercial Nb₂O₅ (entry

Table 3. Performance with different catalyst mixtures

Entry	Ru/C (mg)	Nb ₂ O ₅ (mg)	Conv. (%)	Product Distribution (%)					P _{final} (bar)
				1	2	3	4	5	
1 ^a	0	200	80	-	-	-	4	96	6
2 ^b	0	200	-	-	-	-	-	-	6
3	100	0	96	7.7	8.2	82	2.1	-	14.5
4 ^c	100	0	100	72	-	28	-	-	11.6
5 ^{a,d}	100	200	100	100	-	-	-	-	11

Reaction condition: DHE 0.2 mL, H₂O 12 mL, methanol 0.8 mL, P(H₂) = 6 bar, 250 °C, 12 h. ^a Nb₂O₅ was custom prepared in this laboratory as described in the Experimental section. ^b commercial Nb₂O₅ calcined at 1000 °C. ^c Ru/C was pre-treated in 12 mL H₂O under 10 bar H₂ at 200 °C for 2 h. ^d The same reaction as entry 4 in Table 2.

2, Table 3). One possible explanation may lie in the manner in which the two Nb₂O₅ samples were processed. The commercial sample had been calcined at 1000 °C while the Nb₂O₅ sample prepared in our laboratories and used for catalysis was calcined at 450 °C. Accordingly, we speculated that the higher temperature calcination may have diminished the number of acid sites on Nb₂O₅. This idea was tested by TPD studies of Nb₂O₅ samples that had been first dried and then exposed to ammonia. The amount of NH₃ was absorbed by the Nb₂O₅ sample calcined at 450 °C was 28 mmol per gram of Nb₂O₅ while an analogous sample prepared in this laboratory but calcined at 600 °C only absorbed and released about 2 mmol NH₃ per gram of the sample (SI Figure S-3). Furthermore, the commercial sample absorbed and desorbed essentially no NH₃. Thus, it is clear that higher temperature calcination strongly diminishes the number of acid sites on Nb₂O₅.

When Ru/C alone was used as a catalyst without pretreatment, the major product was propylcyclohexanol (**3**) although about only 8% each of the hydrocarbons (**1**) & (**2**) were formed (entry 3, Table 3). When the Ru/C was first pre-treated by heating under hydrogen to 200 °C, the observed reactivity changed. The major product was propylcyclohexane (**1**) (72%) with the cyclohexanol (**3**) being the remainder (28%) (entry 4, Table 3). Under analogous conditions, the system to which both Ru/C (not activated with H₂) and Nb₂O₅ had been added gave 100% conversion to the propylcyclohexane product exclusively (entry 5, Table 3). Notably, when either form of Ru/C was present, the final pressure in the Parr reactor (after cooling to

RT) was significantly higher than the initial P(H₂). This is apparently due to catalytic reforming of MeOH.

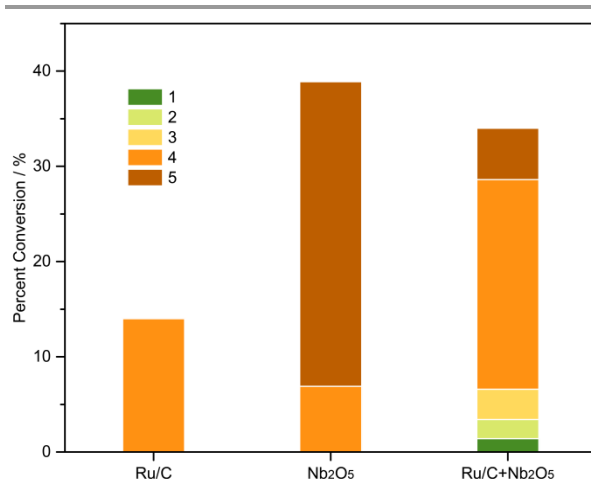
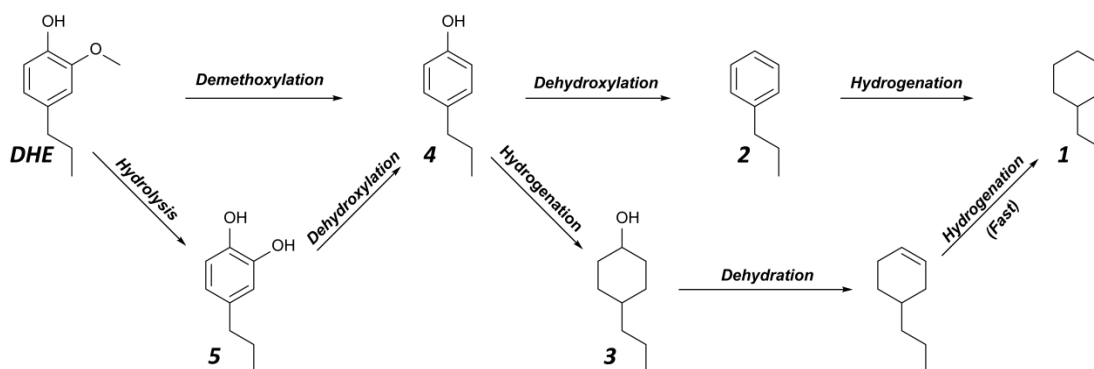


Figure 3. Graphic showing conversion (vertical axis) and product distribution after a 2 h reaction for a mixture of DHE (0.2 mL), H₂O (12 mL), MeOH (0.8 mL) under H₂ (6 bar) with Ru/C (100 mg), Nb₂O₅ (200 mg) or both at 250 °C.

Thus, H₂-pretreated Ru/C can catalyse the HDO/hydrogenation of DHE, although the reaction is more efficient when Nb₂O₅ is present. On the other hand, low T calcined Nb₂O₅ alone only catalysed the conversion of DHE to the



Scheme 1. Possible sequence of reactions leading from DHE to (**1**).

Table 4. Reaction performance in different isotopically labelled reactants

Entry	Water	Methanol	Hydrogen	Conv. (%)	Product Distribution (%)					P _{final} (bar)
					1	2	3	4	5	
1 ^{a,b}	H ₂ O	MeOH	H ₂ (1 bar)	80	3.6	9.5	42	45	-	8
2 ^b	H ₂ O	MeOH	H ₂ (1 bar)	95	42	22	34	2	-	11
3	D ₂ O	methanol-d ₄	H ₂ (1 bar)	54	-	-	-	66	34	6
4 ^c	D ₂ O	methanol-d ₄	H ₂ (1 bar)	85	2.5	5.4	48	44	-	9.7
5	D ₂ O	MeOH	H ₂ (1 bar)	81	1	3.1	11	82	2.3	9.1
6 ^b	H ₂ O	MeOH	H ₂ (6 bar)	100	100	-	-	-	-	11
7 ^d	D ₂ O	methanol-d ₄	H ₂ (6 bar)	100	94	0.1	6.2	-	-	8.9
8	H ₂ O	MeOH	D ₂ (6 bar)	100	61	21	16	2	-	9.6

Conditions: DHE 0.2 mL, Ru/C 100 mg, Nb₂O₅ 200 mg, water 12 mL, methanol 0.8 mL unless noted, purged with H₂ and vented to give P(H₂) = 1 bar, unless noted, 250 °C, 12 h reaction time, unless noted. ^a Methanol 0.4 mL. ^b Entry 1 and entry 2 are the same reactions as entry 2 and entry 3 in Table 1; entry 6 is the same reaction as entry 4 in Table 2. ^c Reaction time 24 h. ^d P(H₂) = 6 bar.

catechol (**5**), presumably the product of hydrolysis of the methoxy group.

The observation that the Ru/C catalyst is more active after pre-treatment suggested that the early stages of the reactions with the physically mixed catalyst would show an induction period while the Ru/C was being activated. This suggestion led to the experiments reported in Figure 3 and SI Table S-1 to examine the products formed by different catalyst combinations over an initial period of 2 h. The take-home lesson from Figure 3 is that, on this time scale, Ru/C alone displays modest activity (14% conversion), but the only product observed was the phenol (**4**), the result of HDO removal of the DHE methoxy group. With Nb₂O₅ alone, conversion was considerably higher, but the primary product was the catechol (**5**). The result with both catalysts illustrates the synergy of this mixture. Although the conversion was about the same as seen with Nb₂O₅ alone, products (**1**), (**2**) and (**3**) are also evident. Scheme 1 suggests a possible sequence of these transformations, with a principal role of the Nb₂O₅ being to catalyse the hydrolysis of the DHE methoxy group to form the catechol (**5**), although, surprisingly, a small amount of the phenol (**4**) was still formed with Nb₂O₅ alone.

Figure 4 illustrates the behaviour of the mixed catalyst system as a function of reaction time. These data confirm the suspected induction period, during which the Ru/C catalyst is activated. After 4 h, all the DHE had been converted to products with 2/3 of the total being the hydrocarbons (**1**) & (**2**). By 8 h, all the products were (**1**) & (**2**) with propyl cyclohexane (**1**) representing an impressive 94 %, while after 12 h only a single product, (**1**), was evident (SI Table S-1). Formation of (**1**) requires HDO of both oxygen containing functional groups of DHE and the hydrogenation of the aromatic ring. Notably, the cyclohexanol (**3**) is observed as an intermediate that presumably undergoes HDO, but none of the direct product of

DHE ring-hydrogenation 4 -propyl-2-methoxy-cyclohexanol was evident.

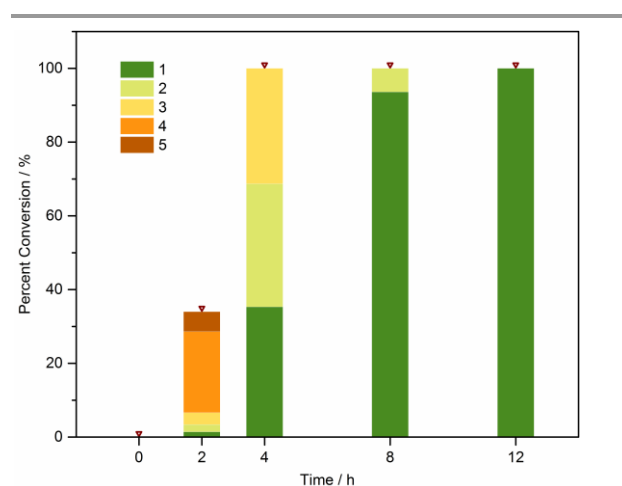


Figure 4. Graphic showing conversion (vertical axis) and product distribution after from 2h, 4h, 8h, 12h reaction for a mixture of DHE (0.2 mL), H₂O (12 mL), MeOH (0.8 mL) under H₂ (6 bar) with Ru/C (100 mg) and Nb₂O₅ (200 mg) at 250 °C.

Reactions of DHE with deuterated reactants

Table 4 summarizes the conversion and products from analogous reactions of DHE in deuterated solvents. Notably, when both D₂O and methanol-d₄ were used instead of the perprotio analogues, there was a significant suppression both of the conversion and of the formation of the more reduced products (**1**), (**2**) and (**3**) with only (**4**) and (**5**) being found (entry 3, Table 4). Extending the reaction time to 24 h did increase production of (**1**), (**2**) & (**3**) with the cyclohexanol (**3**) and the phenol (**4**) now being the major products (entry 4, Table 4). The

pattern was again different when the solvent mixture was D₂O with perprotio MeOH (entry 5, Table 4). The conversion was greater (81%) than when methanol-d₄ was used (54%), and measurable amounts of (1), (2) & (3) were found, but the primary product was (4). Thus, isotope effects are evident in the product distributions from the deuteration of each solvent.

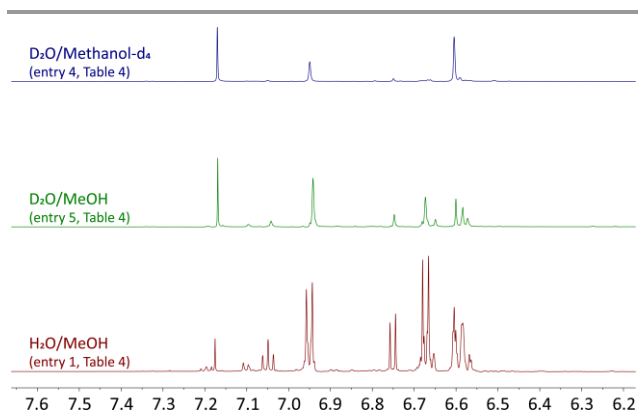


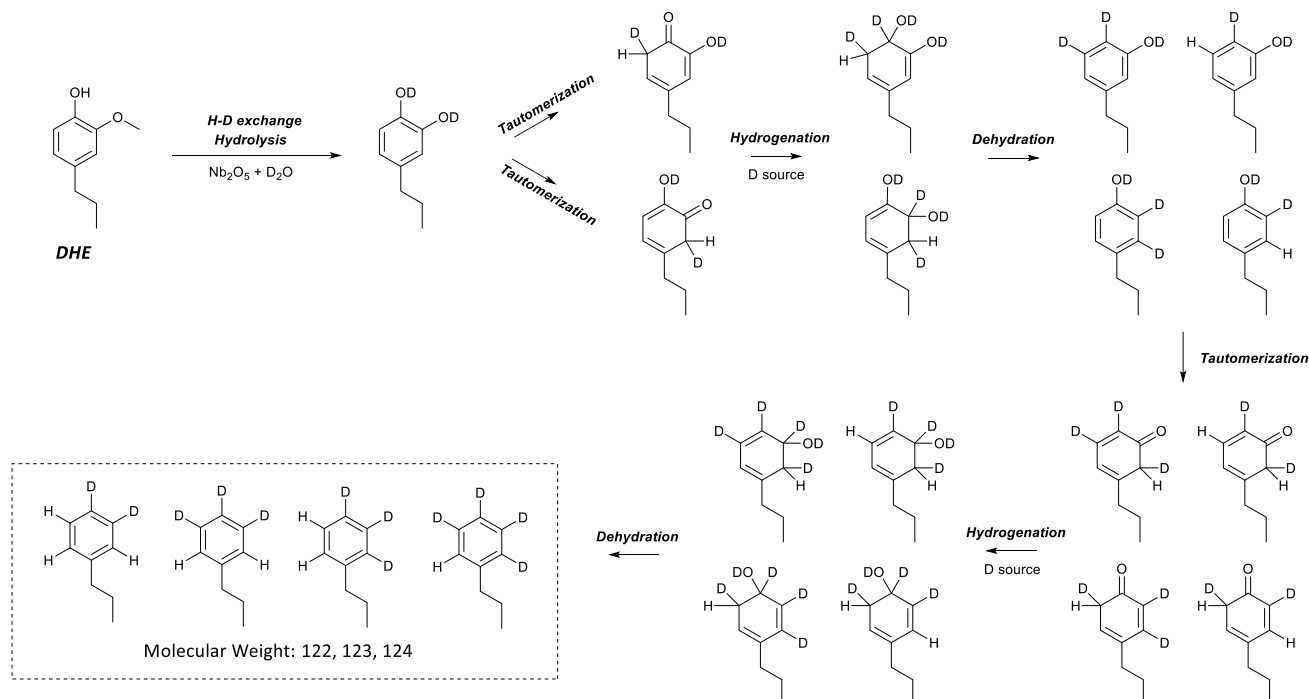
Figure 5. ¹H NMR in the aromatic region of the products obtained after DHE reactions in D₂O/methanol-d₄ (top, entry 4 in Table 4) D₂O/MeOH (middle, entry 5 in Table 4) and H₂O/MeOH (bottom, entry 1 in Table 4)

The DHE reaction with the two catalysts was also run in the D₂O/methanol-d₄ solvent with a higher P(H₂) of 6 bar (entry 7, Table 4). As observed above (entry 6, Table 4), raising the hydrogen pressure substantially accelerated the reaction and improved the selectivity toward (1) to 94% in the deuterated medium.

Figure 5 displays the aromatic regions of the ¹H NMR spectra of products isolated after reactions in H₂O/MeOH (entry 1, Table 4), D₂O/methanol-d₄ (entry 4, Table 4) and D₂O/MeOH (entry 5, Table 4). SI Figure S-4 displays the aliphatic regions of these spectra. A particularly meaningful comparison is between the spectra of entries 1 and 4 in Table 4 since the product distributions for these are very similar with (4) being the primary aromatic product in each case. Simple inspection of these spectra shows that considerable exchange of the aromatic protons with the solvents accompanies the transformation of DHE to the phenolic product (4). Their similar patterns in the aliphatic region indicate the deuterated reactants and solvent have little influence on the exchange of alkyl protons. The ²H NMR spectrum of the product mixture from entry 4 in Table 4 confirms the introduction of both aromatic and aliphatic hydrogens from the deuterated solvent (SI Figure S-5).

The same conclusion can be drawn from the mass spectrum (obtained by GC-MS analysis) of product (2) formed by reaction in D₂O/methanol-d₄ (entry 4, Table 4). The parent MS peak for propylbenzene should appear at mass 120, but the major peak in this region of the MS spectrum (SI Figure S-6) appeared at M/e 123, again indicating that H/D exchange of the aromatic ring occurred prior to ring hydrogenation. Scheme 2 offers a plausible pathway for such exchange via tautomerization of the catechol product (4) formed by hydrolysis of the DHE methoxy group.

The proposed catechol tautomerization mechanism was tested by carrying out the reaction of p-cresol with Nb₂O₅ with D₂O under 6 bar H₂ at 250 °C for 12 h. No HDO of this substrate was observed, but inspection of the aromatic region ²H NMR and mass spectrum of the recovered p-cresol (SI Figure S-7)



Scheme 2. Hypothetical pathways for exchange of aromatic protons with solvent. H-D exchange reaction is very fast in water.

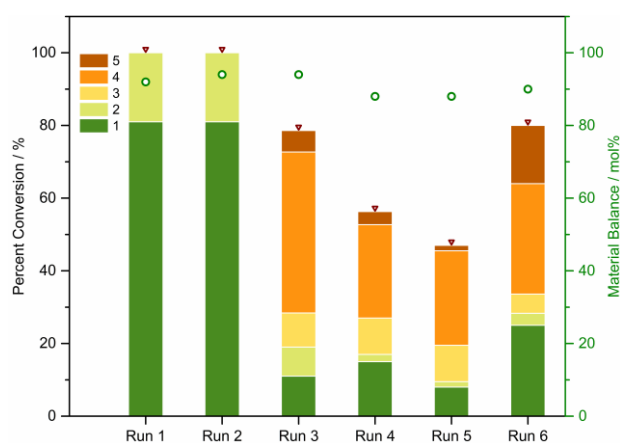
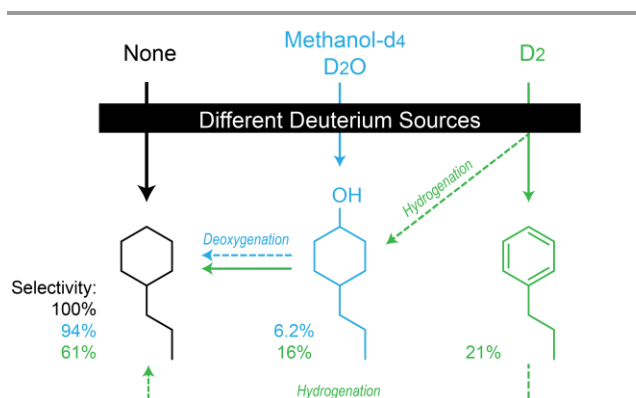


Figure 6. Performance of catalyst reusability. The catalyst mixture was washed twice using ethanol, dried in vacuum chamber at RT for 24 h, and heated in oven at 120 °C for 1 h prior to the next run. For Run 4, catalyst was calcinated under N₂ at 450 °C for another 45 min before use. For Run 5, catalyst was reduced under H₂ (5 %)/Ar at 350 °C for 3 h before use. For run 6, fresh Nb₂O₅ 0.1 g was added to the recovered catalyst (0.2 g remained after run 5). The height of the bar represents the amount of conversion while the small circle represents the material balance of recovered reactant and products which averaged ~91% after workup.

showed that there had been considerable hydrogen exchange with the solvent, as would be expected via tautomerization as illustrated in Scheme 2.

Table 4 also lists the DHE reaction run with the two catalysts in the H₂O/MeOH solvent with D₂ at a pressure of 6 bar (entry 8, Table 4). In this case, the yield of (1) was only 61% as opposed to the 100% selectivity seen under comparable conditions with H₂ (entry 6, Table 4). Products (2) (21%) and (3) (16%) made up the bulk of the other products. Thus, there is a substantial kinetic isotope effect on the HDO and aromatic ring reduction reactions upon replacing H₂ with D₂. The ²H NMR spectrum of the product mixture shows deuterium in the aliphatic region corresponding to (1) and (3) and no deuterium in the aromatic



Scheme 3. The apparent roles of different hydrogen sources.

region (SI Figure S-8), consistent with dihydrogen (H₂/D₂) as the source of aromatic hydrogenation. Scheme 3 outlines the various pathways indicated by these isotope effects.

Catalysis recyclability and stability test

The recyclability of the Ru/C and Nb₂O₅ mixture for DHE conversion was tested in five successive runs (Figure 6 and SI Table S-2). An optimized reaction condition with higher substrate loading (1 mL DHE) and longer reaction time (16 h) was applied to understand the performance of this catalyst mixture. Within the first two runs, 12.5 mmol DHE was fully converted to products (1) (81%) and (2) (19%) (Runs 1 and 2, Figure 6 and SI Table S-2). The conversion of DHE decreased significantly to 78.6%, for run 3. Attempts to reactivate the catalyst mixture by calcining at 450 °C (run 4) or heating under H₂ (run 5) were unsuccessful with conversion dropping to 56%, and 47%, respectively. Thus, the catalyst mixture became less active toward HDO reactions after the second recycle given that propyl phenol (4) was the main product in the last three runs. Overall, the catalyst mixture was able to catalyse 15.06 mmol DHE to fully deoxygenated products (1) and (2) during the first five runs. Notably, the addition of fresh Nb₂O₅ (0.1 g) led to a marked increase in conversion (80%) and yield of hydrocarbon products. For the six runs the material balance of recovered reactant and products averaged 91±3 mol%.

The calculated TON for hydrocarbon production for the first 5 runs was 301 based on the ruthenium (0.05 mmol) or 20 based on the Nb₂O₅ (0.75 mmol) initially present.

Application to a mixture of lignin monomers.

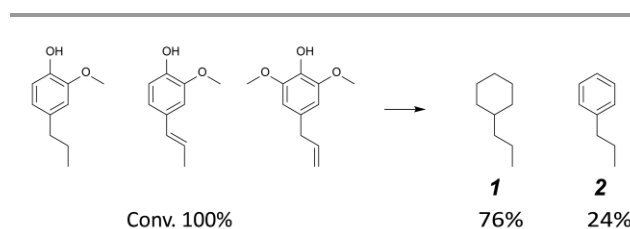


Figure 7. The reaction with a mixture of monolignols: dihydroeugenol (DHE), isoeugenol and 4-allylsyringol. Conditions: 70 μL of each substrate, Ru/C (100 mg), Nb₂O₅ (200 mg), H₂O (12 mL), MeOH (1.2 mL), P(H₂) = 11 bar, 250 °C, 12 h reaction time.

DHE, isoeugenol, and 4-allylsyringol are among the most common lignin monomers. When a mixture of these three substrates (70 μL of each) was subjected to the standard procedure for 12 h, the only products were the hydrocarbons (1) (76%) and (2) (24%) according to GC analysis (Figure 7). Since a 100% yield of (1) can be achieved with an extended reaction time, this system offers a viable new strategy for funnelling the multiple monolignols from lignin disassembly into a much simpler mixture of C₉ alkanes.

in terms of the production of (1), although the product distribution did not match that of a completely fresh catalyst. Thus, a continuous feeding of fresh Nb₂O₅ after the first recycle could improve the total yield of hydrocarbons and maximize the usability of Ru/C catalyst. Ongoing studies will address strategies to minimize catalyst deactivation pathways.

Lastly, subjecting a simulated bio-oil mixture of lignin monomers to the catalyst system optimal for the conversion of DHE, gave a mixture of just the hydrocarbons (1) and (2). Thus, this system provides the opportunity to funnel complex bio-oil mixtures primarily composed of oxygenated lignins to simple C₉ hydrocarbons more compatible with applications as liquid transportation fuels.

Conflicts of interest

The authors have no conflicts to declare.

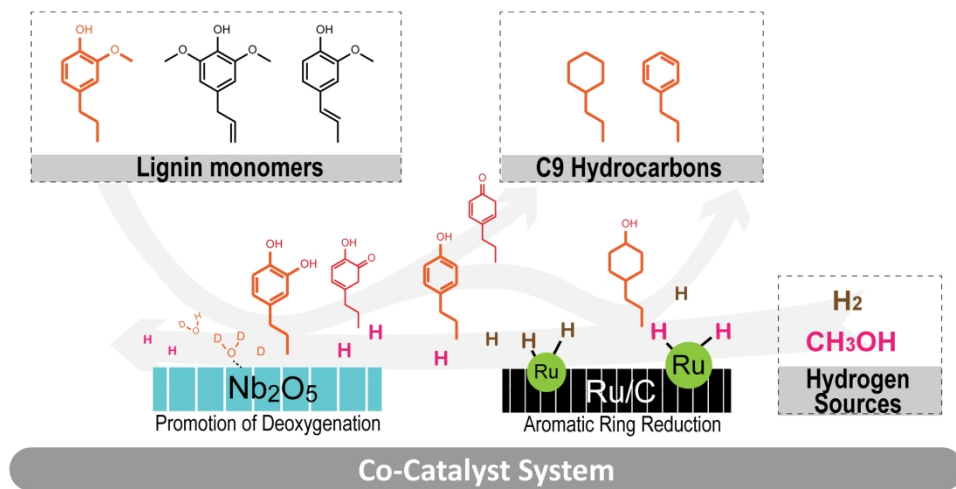
Acknowledgements

This work was supported by the US Department of Energy, Office of Science, Basic Energy Science, award no. DE-SC0019161 (M.M.A.-O.), the Department of Chemistry and Biochemistry, the National Key Technologies R&D Program of China no. 2018YFB1501405, and the Mellichamp Sustainability Initiative at UCSB through a summer fellowship to J.T.

Notes and references

- Barta, K.; Ford, P. C., Catalytic Conversion of Nonfood Woody Biomass Solids to Organic Liquids. *Accounts Chem Res* **2014**, *47* (5), 1503-1512.
- Tuck, C. O.; Perez, E.; Horvath, I. T.; Sheldon, R. A.; Poliakoff, M., Valorization of Biomass: Deriving More Value from Waste. *Science* **2012**, *337* (6095), 695-699.
- Huber, G. W.; Iborra, S.; Corma, A., Synthesis of transportation fuels from biomass: Chemistry, catalysts, and engineering. *Chem Rev* **2006**, *106* (9), 4044-4098.
- Li, C. Z.; Zhao, X. C.; Wang, A. Q.; Huber, G. W.; Zhang, T., Catalytic Transformation of Lignin for the Production of Chemicals and Fuels. *Chem Rev* **2015**, *115* (21), 11559-11624.
- Gallezot, P., Conversion of biomass to selected chemical products. *Chem Soc Rev* **2012**, *41* (4), 1538-1558.
- Hari, T. K.; Yaakob, Z.; Binitha, N. N., Aviation biofuel from renewable resources: Routes, opportunities and challenges. *Renew Sust Energy Rev* **2015**, *42*, 1234-1244.
- Xin, Y.; Jing, Y. X.; Dong, L.; Liu, X. H.; Guo, Y.; Wang, Y. Q., Selective production of indane and its derivatives from lignin over a modified niobium-based catalyst. *Chem Commun* **2019**, *55* (63), 9391-9394.
- Song, W. J.; He, Y. Y.; Lai, S. T.; Lai, W. K.; Yi, X. D.; Yang, W. M.; Jiang, X. M., Selective hydrodeoxygenation of lignin phenols to alcohols in the aqueous phase over a hierarchical Nb₂O₅-supported Ni catalyst. *Green Chem* **2020**, *22* (5), 1662-1670.
- Mäkelä, E.; González Escobedo, J. L.; Neuvonen, J.; Lahtinen, J.; Lindblad, M.; Lassi, U.; Karinen, R.; Puurunen, R. L., Liquid - phase Hydrodeoxygenation of 4 - Propylphenol to Propylbenzene: Reducible Supports for Pt Catalysts. *Chemcatchem* **2020**.
- Kim, H.; Ralph, J., Solution-state 2D NMR of ball-milled plant cell wall gels in DMSO-d(6)/pyridine-d(5). *Org Biomol Chem* **2010**, *8* (3), 576-591.
- Jafarian, S.; Tavasoli, A.; Nikkiah, H., Catalytic hydrotreating of pyro-oil derived from green microalgae spirulina the (*Arthrospira*) *plantensis* over NiMo catalysts impregnated over a novel hybrid support. *Int J Hydrogen Energy* **2019**, *44* (36), 19855-19867.
- Elliott, D. C., Historical developments in hydroprocessing bio-oils. *Energy Fuel* **2007**, *21* (3), 1792-1815.
- Ramesh, A.; Tamizhdurai, P.; Mangesh, V. L.; Palanichamy, K.; Gopinath, S.; Sureshkumar, K.; Shanthi, K., Mg/SiO₂-Al₂O₃ supported nickel catalysts for the production of naphthenic hydrocarbon fuel by hydro-de-oxygenation of eugenol. *Int J Hydrogen Energy* **2019**, *44* (47), 25607-25620.
- Karatzos, S.; van Dyk, J. S.; McMillan, J. D.; Saddler, J., Drop-in biofuel production via conventional (lipid/fatty acid) and advanced (biomass) routes. Part I. *Biofuel Bioprod Bior* **2017**, *11* (2), 344-362.
- Arun, N.; Sharma, R. V.; Dalai, A. K., Green diesel synthesis by hydrodeoxygenation of bio-based feedstocks: Strategies for catalyst design and development. *Renew Sust Energy Rev* **2015**, *48*, 240-255.
- Zhang, J. J.; Zhao, C., A new approach for bio-jet fuel generation from palm oil and limonene in the absence of hydrogen. *Chem Commun* **2015**, *51* (97), 17249-17252.
- Ramesh, A.; Tamizhdurai, P.; Suthagar, K.; Sureshkumar, K.; Theres, G. S.; Shanthi, K., Intrinsic role of pH in altering catalyst properties of NiMoP over alumino-silicate for the vapour phase hydrodeoxygenation of methyl heptanoate. *New J Chem* **2019**, *43* (8), 3545-3555.
- Dong, L.; Shao, Y.; Han, X.; Liu, X. H.; Xia, Q. N.; Parker, S. F.; Cheng, Y. Q.; Daemen, L. L.; Ramirez-Cuesta, A. J.; Wang, Y. Q.; Yang, S. H., Comparison of two multifunctional catalysts [M/Nb₂O₅ (M = Pd, Pt)] for one-pot hydrodeoxygenation of lignin. *Catal Sci Technol* **2018**, *8* (23), 6129-6136.
- Jin, S. H.; Guan, W. X.; Tsang, C. W.; Yan, D. Y. S.; Chan, C. Y.; Liang, C. H., Enhanced Hydroconversion of Lignin-Derived Oxygen-Containing Compounds Over Bulk Nickel Catalysts Though Nb₂O₅ Modification. *Catal Lett* **2017**, *147* (8), 2215-2224.
- Teles, C. A.; de Souza, P. M.; Rabelo-Neto, R. C.; Griffin, M. B.; Mukarakate, C.; Orton, K. A.; Resasco, D. E.; Noronha, F. B., Catalytic upgrading of biomass pyrolysis vapors and model compounds using niobia supported Pd catalyst. *Appl Catal B-Environ* **2018**, *238*, 38-50.
- Zarchin, R.; Rabaev, M.; Vidruk-Nehemya, R.; Landau, M. V.; Herskowitz, M., Hydroprocessing of soybean oil on nickel-phosphide supported catalysts. *Fuel* **2015**, *139*, 684-691.
- He, Z.; Wang, X., Hydrodeoxygenation of model compounds and catalytic systems for pyrolysis bio-oils upgrading. *Catalysis for Sustainable Energy* **2012**, *1*.
- Ding, L. N.; Wang, A. Q.; Zheng, M. Y.; Zhang, T., Selective Transformation of Cellulose into Sorbitol by Using a Bifunctional Nickel Phosphide Catalyst. *ChemSuschem* **2010**, *3* (7), 818-821.
- Wang, H. L.; Yan, S. L.; Salley, S. O.; Ng, K. Y. S., Support effects on hydrotreating of soybean oil over NiMo carbide catalyst. *Fuel* **2013**, *111*, 81-87.
- Alexander, A. M.; Hargreaves, J. S. J., Alternative catalytic materials: carbides, nitrides, phosphides and amorphous boron alloys. *Chem Soc Rev* **2010**, *39* (11), 4388-4401.
- Li, K. L.; Wang, R. J.; Chen, J. X., Hydrodeoxygenation of Anisole over Silica-Supported Ni₂P, MoP, and NiMoP Catalysts. *Energy Fuel* **2011**, *25* (3), 854-863.
- Zhong, X.; Jiang, Y.; Chen, X. L.; Wang, L.; Zhuang, G. L.; Li, X. N.; Wang, J. G., Integrating cobalt phosphide and cobalt nitride-

- embedded nitrogen-rich nanocarbons: high-performance bifunctional electrocatalysts for oxygen reduction and evolution. *J Mater Chem A* **2016**, *4* (27), 10575-10584.
28. Lu, M. H.; Du, H.; Wei, B.; Zhu, J.; Li, M. S.; Shan, Y. H.; Song, C. S., Catalytic Hydrodeoxygenation of Guaiacol over Palladium Catalyst on Different Titania Supports. *Energ Fuel* **2017**, *31* (10), 10858-10865.
29. Kim, M.; Ha, J. M.; Lee, K. Y.; Jae, J., Catalytic transfer hydrogenation/hydrogenolysis of guaiacol to cyclohexane over bimetallic RuRe/C catalysts. *Catal Commun* **2016**, *86*, 113-118.
30. Leal, G. F.; Lima, S.; Graca, I.; Carrer, H.; Barrett, D. H.; Teixeira-Neto, E.; Curvelo, A. A. S.; Rodella, C. B.; Rinaldi, R., Design of Nickel Supported on Water-Tolerant Nb₂O₅ Catalysts for the Hydrotreating of Lignin Streams Obtained from Lignin-First Biorefining. *Iscience* **2019**, *15*, 467-+.
31. Nowak, I.; Ziolk, M., Niobium compounds: Preparation, characterization, and application in heterogeneous catalysis. *Chem Rev* **1999**, *99* (12), 3603-3624.
32. Alharbi, W.; Kozhevnikova, E. F.; Kozhevnikov, I. V., Dehydration of Methanol to Dimethyl Ether over Heteropoly Acid Catalysts: The Relationship between Reaction Rate and Catalyst Acid Strength. *ACS Catal* **2015**, *5* (12), 7186-7193.
33. Guo, T. Y.; Li, X. C.; Liu, X. H.; Guo, Y.; Wang, Y. Q., Catalytic Transformation of Lignocellulosic Biomass into Arenes, 5-Hydroxymethylfurfural, and Furfural. *ChemSuschem* **2018**, *11* (16), 2758-2765.
34. Jehng, J. M.; Wachs, I. E., The Molecular-Structures and Reactivity of Supported Niobium Oxide Catalysts. *Catalysis Today, Vol 8, No 1* **1990**, 37-55.
35. Xia, Q. N.; Cuan, Q.; Liu, X. H.; Gong, X. Q.; Lu, G. Z.; Wang, Y. Q., Pd/NbOPO₄ Multifunctional Catalyst for the Direct Production of Liquid Alkanes from Aldol Adducts of Furans. *Angew Chem Int Edit* **2014**, *53* (37), 9755-9760.
36. Ziolk, M.; Sobczak, I., The role of niobium component in heterogeneous catalysts. *Catal Today* **2017**, *285*, 211-225.
37. Roldugina, E. A.; Naranov, E. R.; Maximov, A. L.; Karakhanov, E. A., Hydrodeoxygenation of guaiacol as a model compound of bio-oil in methanol over mesoporous noble metal catalysts. *Appl Catal a-Gen* **2018**, *553*, 24-35.
38. Wang, X.; Zhu, S. H.; Wang, S.; He, Y.; Liu, Y.; Wang, J. G.; Fan, W. B.; Lv, Y. K., Low temperature hydrodeoxygenation of guaiacol into cyclohexane over Ni/SiO₂ catalyst combined with H beta zeolite. *Rsc Adv* **2019**, *9* (7), 3868-3876.
39. Yu, M. J.; Park, S. H.; Jeon, J. K.; Ryu, C.; Sohn, J. M.; Kim, S. C.; Park, Y. K., Hydrodeoxygenation of Guaiacol Over Pt/Al-SBA-15 Catalysts. *J Nanosci Nanotechnol* **2015**, *15* (1), 527-531.
40. Lee, H.; Kim, H.; Yu, M. J.; Ko, C. H.; Jeon, J. K.; Jae, J.; Park, S. H.; Jung, S. C.; Park, Y. K., Catalytic Hydrodeoxygenation of Bio-oil Model Compounds over Pt/HY Catalyst. *Sci Rep-Uk* **2016**, *6*.
41. Heroguel, F.; Nguyen, X. T.; Luterbacher, J. S., Catalyst Support and Solvent Effects during Lignin Depolymerization and Hydrodeoxygenation. *ACS Sustain Chem Eng* **2019**, *7* (20), 16952-16958.
42. Dong, L.; Xin, Y.; Liu, X. H.; Guo, Y.; Pao, C. W.; Chen, J. L.; Wang, Y. Q., Selective hydrodeoxygenation of lignin oil to valuable phenolics over Au/Nb₂O₅ in water. *Green Chem* **2019**, *21* (11), 3081-3090.
43. Chan, X. J.; Pu, T. C.; Chen, X. Y.; James, A.; Lee, J.; Parise, J. B.; Kim, D. H.; Kim, T., Effect of niobium oxide phase on the furfuryl alcohol dehydration. *Catal Commun* **2017**, *97*, 65-69.
44. Lebarbier, V.; Houalla, M.; Onfroy, T., New insights into the development of Bronsted acidity of niobic acid. *Catal Today* **2012**, *192* (1), 123-129.
45. Michel, C.; Gallezot, P., Why Is Ruthenium an Efficient Catalyst for the Aqueous-Phase Hydrogenation of Biosourced Carbonyl Compounds? *ACS Catal* **2015**, *5* (7), 4130-4132.
46. Duong, N. N.; Aruho, D.; Wang, B.; Resasco, D. E., Hydrodeoxygenation of anisole over different Rh surfaces. *Chinese J Catal* **2019**, *40* (11), 1721-1730.
47. de Souza, P. M.; Rabelo-Neto, R. C.; Borges, L. E. P.; Jacobs, G.; Davis, B. H.; Sooknoi, T.; Resasco, D. E.; Noronha, F. B., Role of Keto Intermediates in the Hydrodeoxygenation of Phenol over Pd on Oxophilic Supports. *ACS Catal* **2015**, *5* (2), 1318-1329.



129x66mm (600 x 600 DPI)